ISSN 0038-0946, Solar System Research, 2024, Vol. 58, No. 4, pp. 367–376. © Pleiades Publishing, Inc., 2024.

New Results of Radiation Study on Board TGO ExoMars in 2018–2023

J. Semkova[a, *], V. Bengin[b, **], R. Koleva[a], K. Krastev[a], Y. Matveychuk[a], B. Tomov[a], N. Bankov[a], S. Malchev[a], Ts. Dachev[a], V. Shurshakov[b], S. Drobyshev[b], I. Mitrofanov[c, *], D. Golovin[c], A. Kozyrev[c], M. Litvak[c], and M. Mokrousov[c]**

[a] *Institute of Space Research and Technology, Bulgarian Academy of Sciences, Sofia, Bulgaria*

[b] *State Scientific Center of the Russian Federation Institute of Medical and Biological Problems, Russian Academy of Sciences, Moscow, Russia*

[c] *Space Research Institute, Russian Academy of Sciences, Moscow, Russia*

**e-mail: jsemkova@stil.bas.bg*

***e-mail: v_benghin@mail.ru*

****e-mail: mitrofanov@np.cosmos.ru*

Received December 12, 2023; revised February 12, 2024; accepted February 16, 2024

Abstract—The article provides a brief description of the Liulin-MO dosimeter, which is part of the FREND (Fine Resolution Epithermal Neutron Detector) device installed on the *TGO* (*Trace Gas Orbiter*) spacecraft of the *ExoMars-2016* mission. Since April 2018, *TGO* has been operating in orbit around Mars. Data are presented on the radiation environment in the orbit of Mars during the decline phase of the 24th cycle of solar activity and the growth phase of the 25th cycle. During the period under review, a maximum flux and dose rate due to galactic cosmic rays (GCR) were observed. Between July 2021 and March 2023, the Liulin-MO dosimeter recorded eight increases in particle fluxes and dose rates from solar proton events (SPEs). Data are presented on the radiation environment during the SPE in Mars orbit in July 2021–March 2022, when Mars was on the opposite side of the Sun from Earth. A comparison is made of particle fluxes measured in orbits around the Earth and Mars.

Keywords: Mars orbit, radiation dose, solar activity, galactic cosmic rays, solar proton events

DOI: 10.1134/S0038094624700291

INTRODUCTION

As is well known (Frank et al., 1965; Grigoriev et al., 1965; National Research Council., 1967; Miroshnichenko and Petrov, 1985), cosmic radiation is one of the unfavorable factors limiting the possibilities of manned flights outside the Earth's magnetosphere. A very large number of publications are devoted to the study of various aspects of the parameters of cosmic radiation and its impact on equipment and living systems. We will note here only a few of them (National Research Council., 1970; Panasyuk and Novikov, 2007; Shafirkin and Grigoriev, 2009; Durante and Cucinotta, 2011). One of the directions was the experimental study of the radiation environment in relation to the task of preparing a manned flight to Mars. There are significantly fewer corresponding experimental data than for near-Earth space. The most significant results are obtained using the RAD instrument on the *MSL* spacecraft (Hassler et al., 2014; Zeitlin et al., 2013; Guo et al., 2015). Using this instrument, characteristics of the radiation environment were obtained during the Earth–Mars flight, as well as on the surface of Mars during operation as part of the *Curiosity* rover (Guo et al., 2017, 2021). The neutron component of radiation during the flight to Mars, in orbit and on the surface of Mars was studied and using observations from the HEND/Mars Odyssey, DAN/MSL instruments (Litvak et al., 2020, 2021; Mitrofanov et al., 2023). The experiment with the Liulin-MO instrument as part of the *ExoMars* TGO space mission, some of the results of which are presented in this article, adds to the very limited experimental data on the parameters of the particle flux and the absorbed dose rate of cosmic radiation in space near Mars. The purpose of research carried out using the Liulin-MO device is:

— Measurement of particle flux, absorbed dose rate, and dose equivalent from galactic and solar cosmic rays, as well as secondary radiation for manned flights in interplanetary space and in orbit around Mars.

— Obtaining data for verification and analysis of radiation environment models and radiation risk assessments for crews of future space missions.

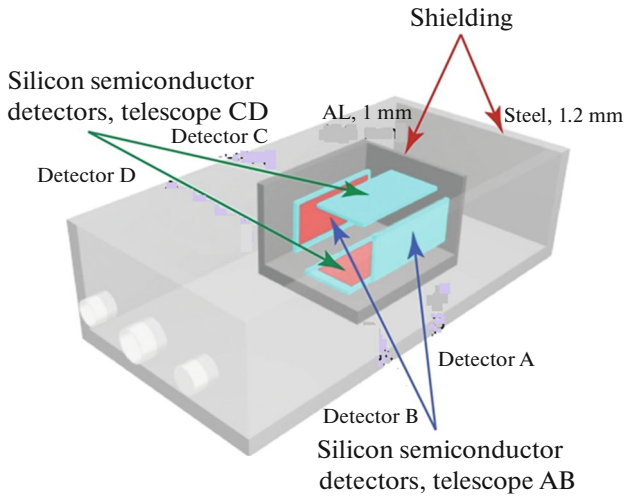

Fig. 1. Schematic representation of the location of detectors in the device Liulin-MO (Semkova and etc., 2021).

Fig. 2. Location of the Liulin-MO dosimeter on the FREND device.

— The *TGO ExoMars* mission provided a unique opportunity to measure the characteristics of cosmic radiation during the decline phase of the 24th and rise phase of the 25th cycle of solar activity.

Descriptions of the *ExoMars* mission, the FREND instrument, which includes the Liulin-MO dosimeter, as well as the Liulin-MO instrument itself and the results obtained with its help were presented in publications (Mitrofanov et al., 2018; Semkova et al., 2018, 2021). In this publication, we present recently obtained results, including measurements during solar proton events (SPEs) in 2021–2023. For ease of perception and to ensure coherence of the presentation, we provide here brief information about the *ExoMars* TGO mission, the FREND device, the design and operating principle of the Liulin-MO device.

DESCRIPTION OF THE LIULIN-MO DEVICE

The *TGO* spacecraft of the Russian-European project *ExoMars* (*Trace Gas Orbiter*) was launched on March 14, 2016. The main task of the project is to register small components of the Martian atmosphere, including methane. One of the objectives of the project is to map the abundance of water in the upper layer of soil, for which the FREND (Fine Resolution Epithermal Neutron Detector) device was included in the *TGO* scientific equipment. The Liulin-MO dosimeter is an integral part of the FREND device. The sensitive elements of the dosimeter are semiconductor detectors. The device contains four silicon detectors with an area of 2 cm^2, thickness 300 microns. The detectors are placed in such a way that they form two pairs of detectors located one opposite the other, as shown in Fig. 1.

Each pair of detectors located opposite each other forms a telescope, which allows, when the detector signals are turned on for coincidence, selecting from the entire stream of registered particles only those whose direction of motion does not deviate greatly from the direction of the normal to the detectors. In each telescope, one detector ensures registration of energy releases of particles with relatively small ionization losses, and the second, large ones. Signals from the detectors are fed to preamplifiers, processing logic circuits, amplitude-to-digital converters and a microcontroller. Information from the microcontroller is transmitted to the FREND device and then through the spacecraft systems to Earth. A detailed description of the Liulin-MO device and the logic of its operation are presented in the publication (Semkova et al., 2018). The output information of the device is the number of particles and the total energy release in each of the detectors, recorded every minute, as well as the energy release spectra in the detectors, recorded every hour. In addition, the values of the number of particles and energy releases in the detectors are also recorded for particles that coincided in pairs of detectors forming the telescope.

The shielding of detectors from different directions is extremely heterogeneous. And it is very significant for the conditions for recording radiation.

The Liulin-MO device is mounted directly under the collimator of the FREND device, as shown in Fig. 2. Its shielding from the bottom is quite significant, and from the opposite side it is determined only by the structural elements of the Liulin-MO itself.

The shielding of the detectors was calculated based on documentation for the Liulin-MO and FREND instruments, as well as data on the ExoMars design. Distribution covers the range from 0.9 to 178 g/cm^2.

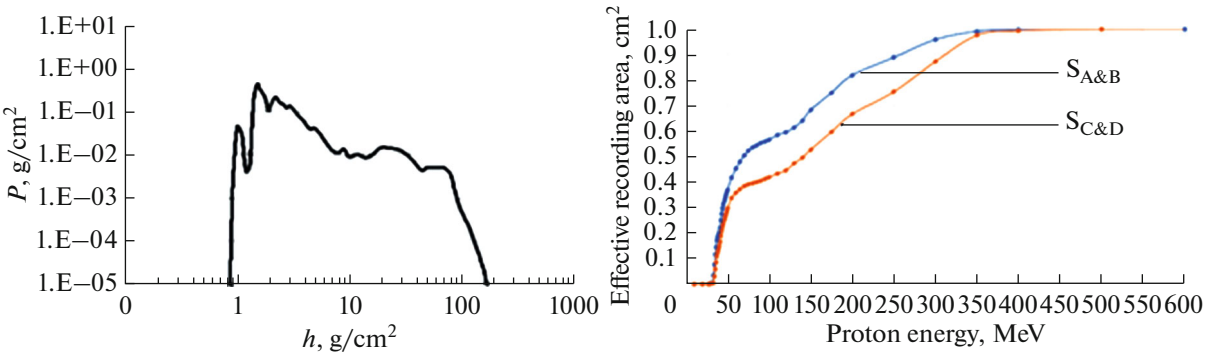

Fig. 3. Shielding distribution functions of detectors (left panel) and the corresponding dependences of the effective detection area of protons on their energy (right panel).

Based on the resulting distribution, the detector shielding function was calculated, which is the probability density P encounter a shielding thickness equal to the function argument when moving in a randomly chosen direction. This distribution of shielding thickness corresponds to the dependence of the effective detection area of protons on their energy. The shielding functions of detectors and the corresponding dependences of the effective detection area of protons on their energy are presented in Fig. 3. The minimum proton energy that can be detected is 27 MeV. However, as can be seen from the graph, a noticeable detection efficiency appears starting from a proton energy of 45–50 MeV.

MEASUREMENT RESULTS

Data Obtained from Liulin-MO

Measurements taken during the Earth–Mars flight. In the period from April 22, 2016, to September 15, 2016, the Liulin-MO device was turned on periodically.

Data obtained from the highly elliptical orbit MCO1. Orbital parameters: altitude 98 000 ± 230 km, inclination 0°, orbital period 4.2 sol (Martian days). The *TGO* arrived in this orbit on October 19, 2016. The FREND instrument (and Liulin-MO) was turned on during the period October 31, 2016–January 17, 2017.

Data obtained from the highly elliptical orbit MCO2. Orbital parameters: altitude 37 150 ± 200 km, inclination 74°, orbital period 24 hours 39 min. The FREND device (and Liulin-MO) was turned on from February 24, 2017, to March 7, 2017.

Measurements taken in "scientific" orbit around Mars. Orbital parameters: almost circular orbit with an altitude of about 400 km, inclination 74°, orbital period about 2 hours. In this orbit, the Liulin-MO instrument has been operating almost continuously since April 16, 2018.

In Fig. 4, the periods of measurements with the Liulin-MO device are compared with the level of solar activity (SA). Data on the number of sunspots presented in the figure are taken from the website http://sidc.be/silso, the Royal Observatory of Belgium. The results obtained during the first three stages of the *TGO* flight were reviewed in (Semkova et al., 2018). In this publication we will consider the results obtained in the "scientific" orbit. Figure 5 shows graphs of average daily fluxes and dose rates measured by the Liulin-MO device from May 2018 to September 2023.

The top graph shows particle flux data, and the bottom graph shows radiation dose rates. Data are presented for each detector pair AB and CD.

One can see the maximum flux occurring at the SA minimum, as well as the subsequent decrease in readings due to the effect of solar modulation of the GCR. The increase in dose rate from May 2018 to February 2020 corresponds to an increase in GCR intensity during the decline of the 24th solar cycle. In March–August 2020, radiation parameters were at their maximum, which was due to the minimum of the 24th cycle and the transition to the 25th cycle of solar activity. The maximum flow value was 3.3 particles cm^{-1} s^{-1}, absorbed dose rate (in silicon) 382 microGray per day, dose equivalent rate 1700 microSievert per day. Since September 2020, a decrease in GCR flux and dose rate has been observed. Between September 2020 and September 2023, the GCR flux, absorbed dose rate, and dose equivalent rate decreased by 47% relative to the values measured during the solar cycle 24 minimum.

Since 2021, increases in fluxes and radiation dose rates have been observed, caused by the arrival of protons from large solar flares in the vicinity of Mars. Eight such increases due to SPE were recorded, data on which are presented in Table 1.

The solar proton event observed on February 15–19, 2022, was the most intense recorded by the Liulin-MO instrument in Mars orbit. The absorbed dose for an event approximately corresponds to the dose for 38 days of flight under undisturbed radiation conditions, and the dose equivalent corresponds to the dose for 13 days of flight under undisturbed conditions. The dose from SPE October 28–31, 2021, is approximately two

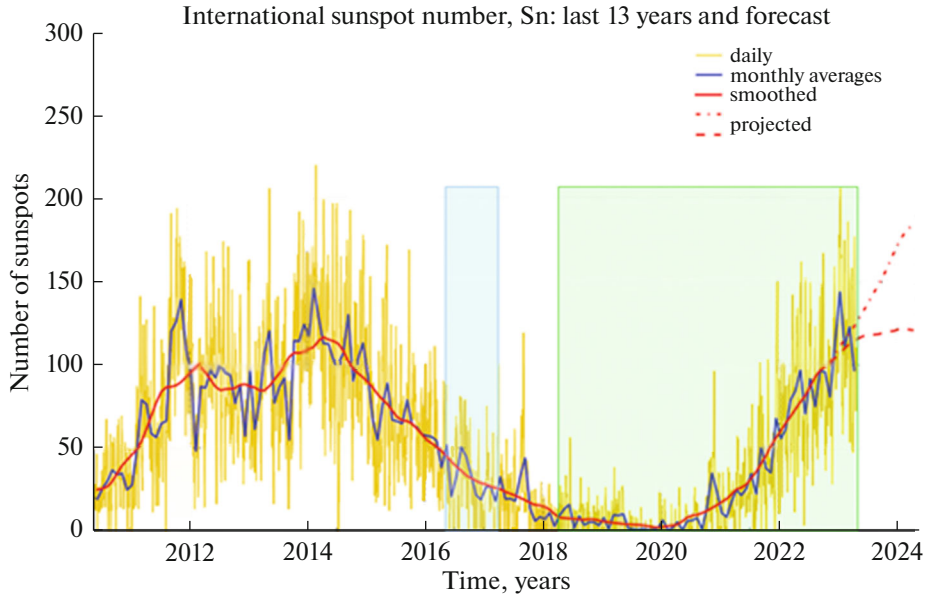

Fig. 4. Solar activity during the periods of measurement by the Liulin-MO device. The shaded areas show the periods of Liulin-MO measurements: on the flight path, MSO1 and MSO2 in the left rectangle, and in the scientific, circular orbit of Mars in the right rectangle.

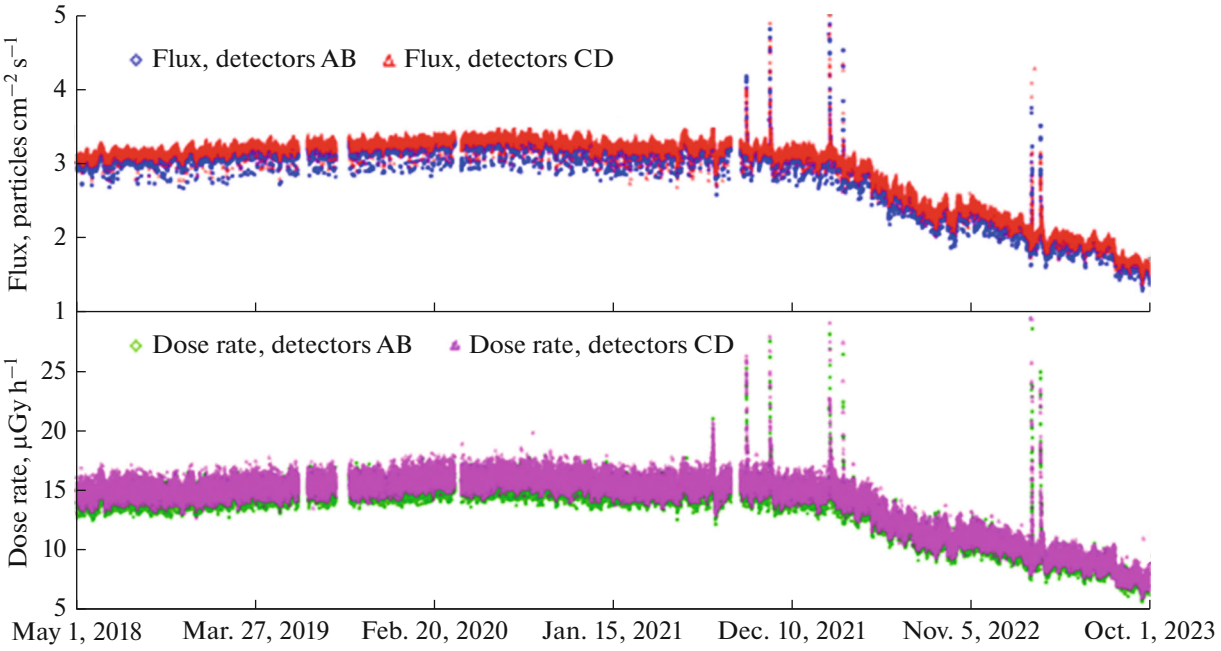

Fig. 5. Graphs of average particle fluxes and radiation dose rates measured by the Liulin-MO device.

times less. The remaining SPEs gave significantly lower doses. Let us look at the events of October 28, 2021, and February 15, 2022, in more detail.

The event on October 28, 2021, is compared to an X1.0 class solar flare that occurred at 15:17 UT in active region 12891 with coordinates S26W05. The data is taken from the SPE catalog posted on the space weather website of the SINP MSU https://swx.sinp.msu.ru/apps/sep_events_cat. Figure 6 shows the relative positions of the Sun, Earth, and Mars, as well as the corresponding interplanetary magnetic field lines, calculated in the approximation of a constant solar wind speed of 400 km/s. The figure was obtained using the site https://solar-machgithub.io, which provides cal-

Table 1. SPE recorded by the Liulin-MO instrument in Mars orbit

Event start time, UT	Duration, h	Total dose per SPE (in silicon), milliGray	Maximum dose rate, microGray h^{-1}	Maximum flow, $cm^{-2}\ s^{-1}$
July 17, 2021, 09:06 am	23	0.096	20	4.25 ± 0.2
September 17, 2021, 07:12 am	37	0.185	26	4.5 ± 0.2
October 28, 2021, 4:55 pm	79	6.500	402	48.5 ± 2.43
February 15, 2022, 11:00 pm	76	13.800	1009	109.7 ± 5.5
March 14, 2022, 5:55 pm	17	0.095	31	5.13 ± 0.26
February 24, 2023, 9:07 pm	24	0.185	59	5.1 ± 0.25
February 25, 2023, 9:20 pm	21	0.098	47	3.9 ± 0.2
March 13, 2023, 05:24 am	39	0.165	38	4.4 ± 0.22

Table 2. Dose values reported during SPE October 28, 2021

Device	Location of measurements	Dose (in water) per SPE, microGray
RAMIS	In polar orbit near Earth	10474
LND	On the lunar surface	17404
CRaTER	In lunar orbit	31 191
RAD	On the surface of Mars	288
Liulin-MO	In orbit around Mars	9186

culations in accordance with the methodology described in (Gieseler et al., 2022).

You can see that Mars and Earth are located on almost opposite sides of the Sun. However, the fluxes of protons generated by this event were observed at both of these points in the Solar System almost simultaneously. Figure 7 compares the time dependences of the flux of protons with energies greater than 50 MeV, recorded near the Earth on the *GOES-16* spacecraft, and the flux of particles measured by a pair of detectors A and B of the Liulin-MO instrument near Mars. *GOES-16* data were also taken from the space weather website of the Institute of Nuclear Physics of Moscow State University (section "INSTRUMENTS") https://swx.sinp.msu.ru/tools/ida.php?gcm=1.

It can be seen that the increase in flows near the Earth begins a little earlier and has a steeper growth front. During the phase of decreasing intensity, the appearance of the second and third local maxima is observed almost simultaneously near the Earth and Mars.

During the SPE on October 28, 2021, cosmic radiation doses were recorded on several spacecraft at once: in polar orbit near Earth with the RAMIS instrument, on the lunar surface with the LND instrument and in lunar orbit with the CRaTER instrument, on the surface of Mars with the RAD instrument and in orbit around Mars with the Liulin-MO instrument (Guo et al., 2023). Figure 8 presents dose rate data taken from this work, measured with these devices, as well as the dynamics of dose accumulation during SPE. Table 2 shows the values of doses in water accumulated over the entire event.

The next, largest event recorded by the Liulin-MO instrument occurred on February 15, 2022. This event is associated with a powerful coronal mass ejection (CME), which was observed on several coronagraphs located on the SOHO, STEREO-A and the *Solar Orbiter* spacecraft (https://www.esa.int/Science_Ex-

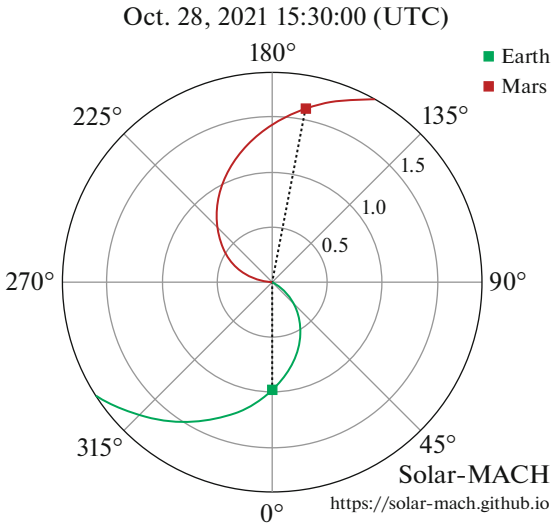

Fig. 6. The relative position of the Sun, Earth, Mars and model interplanetary magnetic field lines connecting the Earth and Mars with the Sun on October 28, 2021.

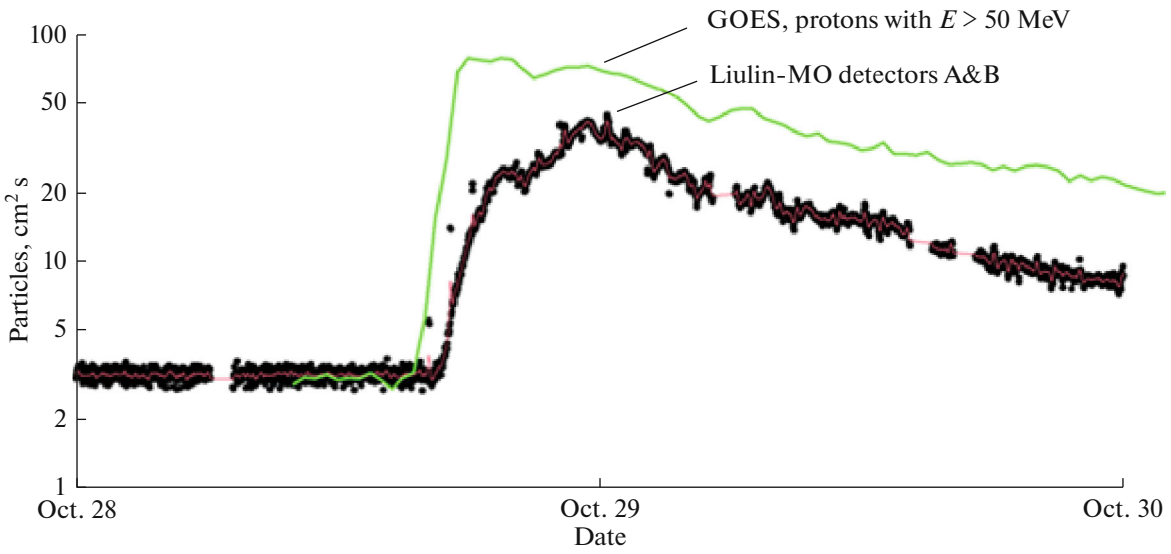

Fig. 7. Time dependence of the proton flux near the Earth and the particle flux measured near Mars. The curve is the flux of protons with energies greater than 50 MeV recorded near the Earth by the GOES-16 spacecraft. The dots are the particle flux measured by a pair of detectors A and B of the Liulin-MO instrument near Mars.

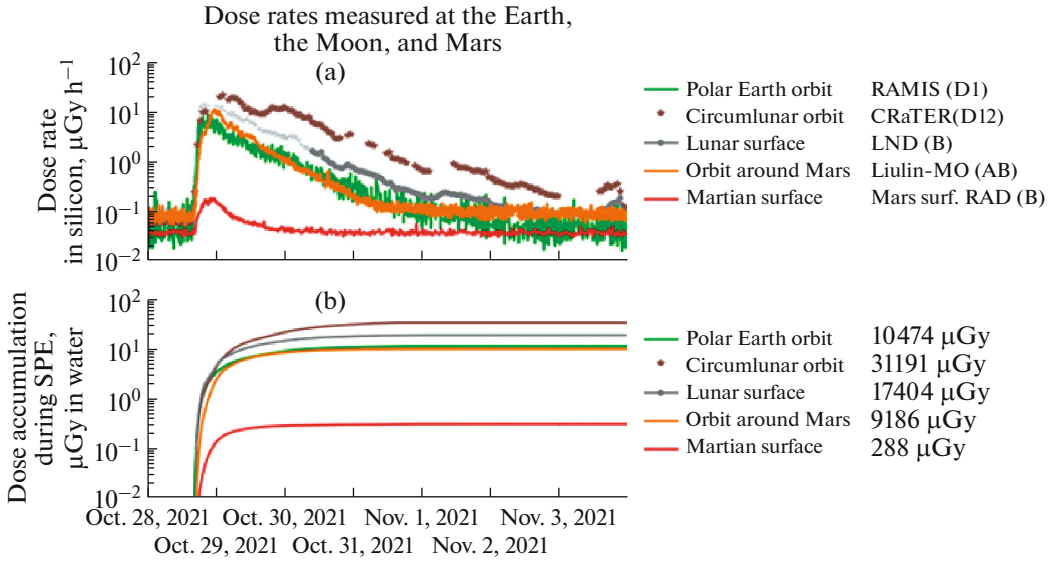

Fig. 8. Dose rates in silicon (top panel) and accumulated doses in water from solar energetic particles (bottom panel) measured at various locations in the Solar System during the October 28, 2021 SPE. Data taken from (Guo et al., 2023). The designations from bottom to top correspond to: the RAD instrument operating on the surface of Mars, the Liulin-MO instrument in orbit around Mars, the RAMIS instrument operating in polar orbit near the Earth, the LND instrument operating on the lunar surface, the CRaTER instrument in lunar orbit.

ploration/Space_Science/Solar_Orbiter/Giant_solar_eruption_seen_by_Solar_Orbiter). To relate observed SPEs in Mars orbit to solar events, we use information provided in the CME listings in online catalogs: Solar Eruptive Event Detection System (SEEDS, http://spaceweather.gmu.edu/seeds/) and CDAW Catalog (https://cdaw.gsfc.nasa.gov/CME_list/) (Gopalswamy et al., 2009). SEEDS uses images from the LASCO coronagraph on the *SOHO* spacecraft (Brueckner et al. 1995), from the C2 telescope and the external coronagraph COR2 (Howard et al., 2002) onboard the *STEREO* spacecraft. The CDAW catalog uses images obtained from the LASCO, C2 and C3 telescopes on the *SOHO* spacecraft.

These data show that the CME occurred beyond the eastern limb and propagated in a northeasterly direction on the far side of the Sun at a speed of about

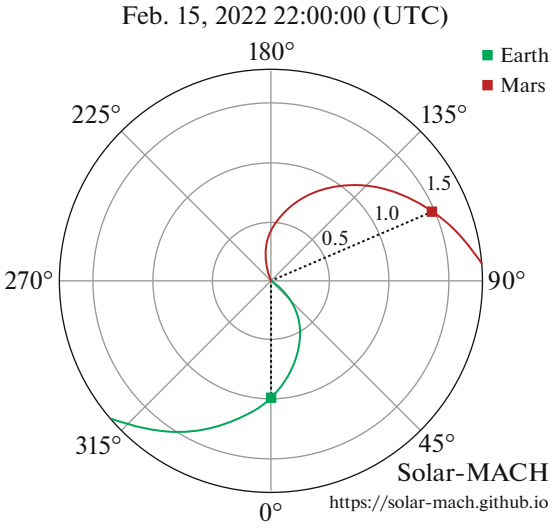

Fig. 9. The relative position of the Sun, Earth, Mars and model interplanetary magnetic field lines connecting the Earth and Mars with the Sun on February 15, 2022.

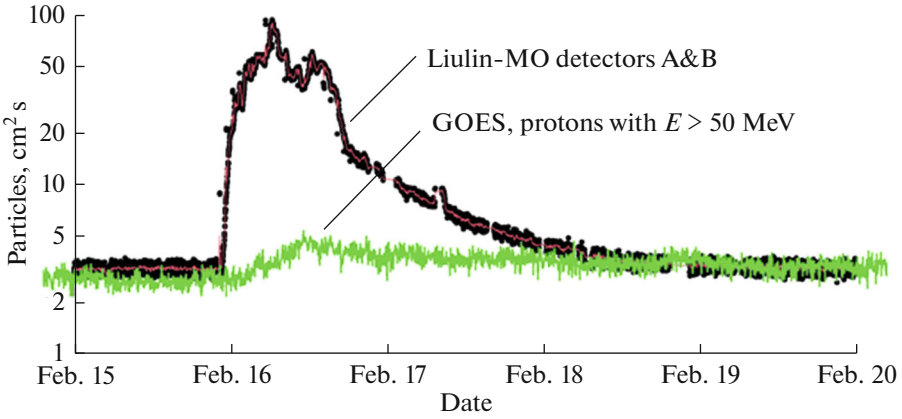

Fig. 10. Comparison of particle fluxes recorded by the *GOES* and *ExoMars* spacecraft during the SPE on February 15, 2022. The curve is the flux of protons with an energy greater than 50 MeV recorded near the Earth by the *GOES-16* spacecraft. The dots are the particle flux measured by a pair of detectors A and B of the Liulin-MO instrument near Mars.

1900 km s^{-1}. It can be assumed that the acceleration of protons to high energies occurred at the front of the shock wave of this CME. The relative position of the Sun, Earth, Mars, and the interplanetary magnetic field lines connecting the Earth and Mars with the Sun on February 15, 2022, is shown in Fig. 9.

It can be seen that in this event the flux of particles near Mars significantly exceeded the flux of particles near the Earth (Fig. 10). This is due to the more convenient location of Mars relative to the supposed area of acceleration of high-energy protons. Both of the SPEs examined occurred under conditions where the Earth and Mars were in almost opposite directions relative to the Sun.

On February 24 and 25, 2023, SPEs occurred, during which the Earth and Mars were on the same side of the Sun on close interplanetary magnetic field lines, as shown in Fig. 11.

Both solar flares occurred in active region 13229. The first M3.7 class flare occurred on February 24 at 20:03 in the area with coordinates N29W24. The second M6.4 class flare occurred on February 25 at 18:40 in the area with coordinates N24W45. Despite the fact that both flares were relatively weak, their appearance near the base of the corotating field line of the interplanetary magnetic field contributed to the appearance of high-energy protons in the vicinity of Earth and Mars. Figure 12 shows the time profiles of proton fluxes with energies greater than 50 MeV and greater than 100 MeV, recorded near the Earth on the *GOES-16* spacecraft, as well as the particle flux measured by a

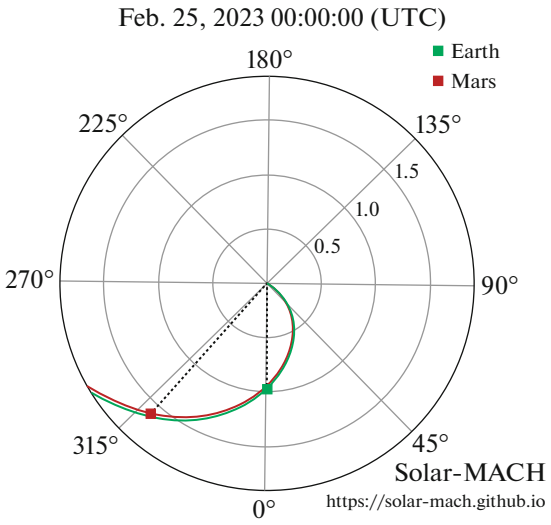

Fig. 11. The relative position of the Sun, Earth, Mars and model interplanetary magnetic field lines connecting the Earth and Mars with the Sun on February 24 and 25, 2023.

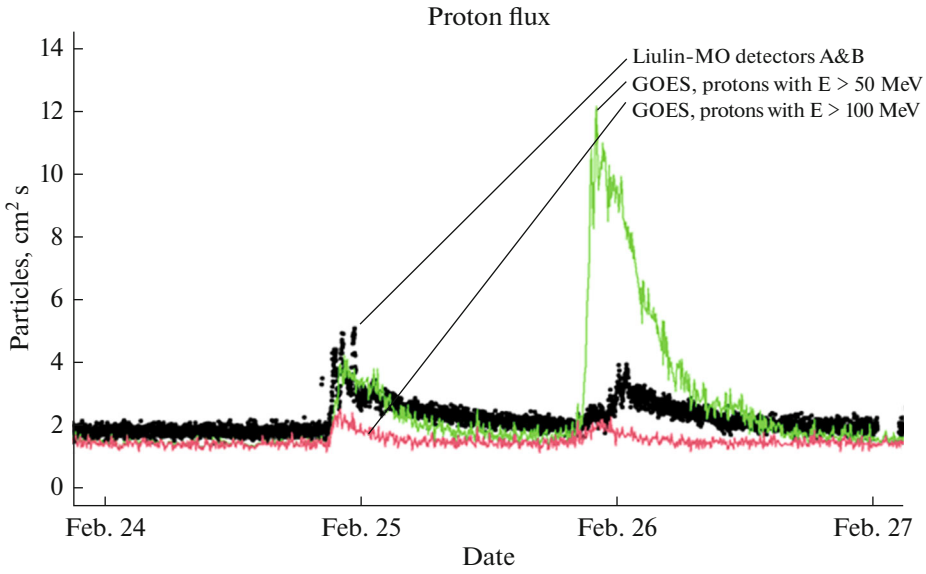

Fig. 12. Comparison of particle fluxes recorded by the *GOES-16* and *ExoMars* spacecraft during the SPE on February 24–25, 2023. The curves are fluxes of protons with energies greater than 50 MeV and greater than 100 MeV, respectively, recorded near the Earth by the *GOES-16* spacecraft. The dots are the particle flux measured by a pair of detectors A and B of the Liulin-MO instrument near Mars.

pair of detectors A and B of the Liulin-MO instrument near Mars.

It can be seen that the energy spectrum of the second SPE is much softer than that of the first. The beginning of the flux increase for the first event near the Earth and Mars occurs almost simultaneously, and for the second event there is a delay in the maximum flux near Mars, compared to the moment the maximum occurs near the Earth. The presented results are important for subsequent analysis of the processes of propagation of solar cosmic rays in interplanetary space.

CONCLUSIONS

Unique data were obtained on the radiation environment in the orbit of Mars during the decline phase of the 24th cycle of solar activity and the growth phase of the 25th cycle. It is shown that in September 2023, the GCR flux, absorbed dose rate and dose equivalent

rate are 47% relative to the values measured during the minimum period of the 24th cycle of solar activity.

Unique data were also obtained on the radiation environment during the SPE in Mars orbit in July 2021–March 2022, when Mars was on the opposite side of the Sun from Earth. A comparison is made of particle fluxes measured in orbits around the Earth and Mars.

Between July 2021 and March 2023, the Liulin-MO instrument at TGO detected eight increases due to solar proton events. Six of them were minor.

Two SPEs: October 28, 2021, and February 15, 2022, gave a noticeable contribution to the dose of 6.5 milliGrays and 13.8 milliGrays in silicon, respectively.

The Liulin-MO device data used in this work is freely available on the website http://esa-pro.space.bas.bg/LIULIN_MO_MARS_2/.

The results obtained are important for experimental verification and improvement of methods for calculating and predicting the radiation environment when planning manned expeditions beyond the Earth's magnetosphere.

FUNDING

The work of the Russian coauthors was carried out within the framework of the Basic Scientific Research Program of the Russian Academy of Sciences no. FMFR-2024-0036. At IKI RAS, work was carried out within the framework of project No. 23-12-0032 of the Russian Science Foundation.

CONFLICT OF INTEREST

The authors of this work declare that they have no conflicts of interest.

REFERENCES

Brueckner, G.E., Howard, R.A., Koomen, M.J., Korendyke, C.M., Michels, D.J., Moses, J.D., Socker, D.G., Dere, K.P., Lamy, P.L., Llebaria, A., and 5 co-authors, The Large Angle Spectroscopic Coronagraph (LASCO), *Sol. Phys.,* 1995, vol. 162, pp. 357–402. https://doi.org/10.1007/BF00733434

Durante, M. and Cucinotta, F.A., Physical basis of radiation protection in space travel, *Rev. Modern Phys.,* 2011, vol. 83, no. 4, pp. 1245–1281.

Frank, G.M., Saksonov, P.P., Antipov, V.V., and Dobrov, N.N., Radiobiological problems of space flights, in *Proc. Ist Int. Symp. on "Basic Environmental Problems of Man in Space," Paris, 1962,* Bjurstedt, H., Eds., Wien–New York: Springer Sci., 1965, pp. 254–266.

Gieseler, J., Dresing, N., Palmroos, C., von Forstner, J.L.F., Price, D.J., Vainio, R., Kouloumvakos, A., Rodríguez-García, L., Trotta, D., Génot, V., Masson, A., Roth, M., and Veronig, A., Solar-MACH: An open-source tool to analyze solar magnetic connection configurations, *Front. Astron. Space Sci.,* 2022, vol. 9. https://doi.org/10.3389/fspas.2022.1058810

Gopalswamy, N., Yashiro, S., Michalek, G., Stenborg, G., Vourlidas, A., Freelan, S., and Howard, R., The SOHO/LASCO CME Catalog, *Earth, Moon, and Planets,* 2009, vol. 104, pp. 295–313. https://doi.org/10.1007/s11038-008-9282-7

Grigoriev, Yu., Guskova, A.K., Domshlak, M., Wysocki, V.G., Raevskaya, S.A., Markelov, B.A., and Darenskay, N., The problem for establish of a limits doses to cosmonauts, in *Proc. XVI Int. Astronautical Congress, Athens,* Sept. 13–18, 1965, vol. 4, pp. 145–161.

Guo, J., Zeitlin, C., Wimmer-Schweingruber, R.F., Rafkin, S., Hassler, D.M., Posner, A., Heber, B., Köhler, J., Ehresmann, B., Appel, J.K., and 8 co-authors, Modeling the variations of dose rate measured by RAD during the first MSL Martian year: 2012–2014, *Astrophys. J.,* 2015, vol. 810, no. 1, id. 24.

Guo, J., Zeitlin, C., Wimmer-Schweingruber, R., Hassler, D.M., Köhler, J., Ehresmann, B., Böttcher, S., Böhm, E., and Brinza, D.E., Measurements of the neutral particle spectra on Mars by MSL/RAD from 2015-11-15 to 2016-01-15, *Life Sci. Space Res.,* 2017, vol. 14, pp. 12–17.

Guo, J., Zeitlin, C., Wimmer-Schweingruber, R.F., Hassler, D.M., Ehresmann, B., Rafkin, S., von Forstner, F.J.L., Khaksarighiri, S., Liu, W., and Wang, Y., Radiation environment for future human exploration on the surface of Mars: The current understanding based on MSL/RAD dose measurements, *Astron. Astrophys. Rev.,* 2021, vol. 29, no. 1, pp. 1–81. https://doi.org/10.1007/s00159-021-00136-5

Guo, J., Li, X., Zhang, J., Dobynde, M.I., Wang, Y., Xu, Z., Berger, T., Semkova, Y., Wimmer-Schweingruber, R.F., Hassler, D., Zeitlin, C., Ehresmann, B., Matthiä, D., and Zhuang, B., The first ground level enhancement seen on three planetary surfaces: Earth, Moon, and Mars, *Geophys. Res. Lett.,* 2023, vol. 50, no. 15, p. 2023GL103069. https://doi.org/10.1029/2023GL103069

Hassler, D.M., Zeitlin, C., Wimmer-Schweingruber, R.F., Ehresmann, B., Rafkin, S., Eigenbrode, J.L., Brinza, D.E., Weigle, G., Böttcher, S., Böhm, E., and 14 co-authors, Mars' surface radiation environment measured with the Mars Science Laboratory's Curiosity rover, *Science,* 2014, vol. 343, no. 6169, id. 1244797. https://doi.org/10.1126/Science.1244797

Howard, R.A., Moses, J.D., Socker, D.J., Dere, K.P., Cook, J.W., and SECCHI Consortium, Sun Earth Connection Coronal and Heliospheric Investigation (SECCHI), *Adv. Space Res.,* 2002, vol. 29, no. 12, pp. 2017–2026. https://doi.org/10.1016/S0273-1177(02)00147-3

Litvak, M.L., Sanin, A.B., Mitrofanov, I.G., Bakhtin, B., Jun, I., Martinez-Sierra, L.M., Nosov, A., and Perkhov, A.S., Mars neutron radiation environment from HEND/Odyssey and DAN/MSL observations, *Planet. Space Sci.,* 2020, vol. 184, p. 104866. https://doi.org/10.1016/j.pss.2020.104866

Litvak, M.L., Mitrofanov, I.G., Sanin, A.B., Bakhtin, B., Golovin, D.V., and Zeitlin, C., Observations of neutron radiation environment during Odyssey cruise to Mars, *Life Sci. Space Res.,* 2021, vol. 29, pp. 53–62. https://doi.org/10.1016/j.lssr.2021.03.003

Miroshnichenko, L.I. and Petrov, V.M., *Dinamika radiatsionnykh usloviy v kosmose* (Dynamics of Radiation

Conditions in Space), Moscow: Energoatomizdat, 1985.

Mitrofanov, I., Maklahov, A., Bakhtin, B., Golovin, D., Kozyrev, A., Litvak, M., Mokrousov, M., Sanin, A., Tretyakov, V., Vostrukhin, A., and 12 co-authors, Fine Resolution Epithermal Neutron Detector (FREND) onboard the Trace Gas Orbiter, *Space Sci. Rev.,* 2018, vol. 214, p. 86. .
https://doi.org/10.1007/s11214-018-0522-5

Mitrofanov, I.G., Litvak, M.L., Sanin, A.B., Semkova, I.V., and Dachev, Ts.P., Estimation of the neutron component of the radiation background in the Gale Crater on Mars, *Sol. Syst. Res.,* 2023, vol. 57, no. 3, pp. 191–199.
https://doi.org/10.31857/S0320930X2303007

National Research Council, *Radiobiological Factors in Manned Space Flight,* Washington, DC: The National Academies Press, 1967.
https://doi.org/10.17226/12407

National Research Council, *Radiation Protection Guides and Constraints for Space-Mission and Vehicle-Design Studies Involving Nuclear Systems,* Washington, DC: The National Academies Press, 1970.
https://doi.org/10.17226/12393

Physical conditions in outer space, in *Model' kosmosa: Nauchno-informatsionnoye izdaniye (Model of Space: Scientific Information Publication)*, Panasyuk, M.I. and Novikov, L.S., Eds., Moscow, 2007, vol. 1, ch. 3, pp. 417–667.

Semkova, J., Koleva, R., Benghin, V., Dachev, T., Matviichuk, Yu., Tomov, B., Krastev, K., Maltchev, St., Dimitrov, P., Mitrofanov, I., and 14 co-authors, Charged particles radiation measurements with Liulin-MO dosimeter of FREND instrument aboard ExoMars Trace Gas Orbiter during the transit and in high elliptic Mars orbit, *Icarus,* 2018, vol. 303, pp. 53–66.
https://doi.org/10.1016/j.icarus.2017.12.034

Semkova, J., Koleva, R., Benghin, V., Dachev, T., Matviichuk, Yu., Tomov, B., Krastev, K., Maltchev, S., Dimitrov, P., Bankov, N., and 12 co-authors, Results from radiation environment measurements aboard ExoMars Trace Gas Orbiter in Mars science orbit in May 2018–December 2019, *Icarus,* 2021, vol. 361, p. 114264.
https://doi.org/10.1016/j.icarus.2020.114264

Shafirkin, A.V. and Grigor'ev, Yu.G., *Mezhplanetnyye i orbital'nyye polety. Radiatsionnyy risk dlya kosmonavtov. Radiobiologicheskoye obosnovaniye* (Interplanetary and Orbital Flights. Radiation Risk for Astronauts. Radiobiological Substantiation), Moscow: *Ekonomika*, 2009.

Zeitlin, C., Hassler, D.M., Cucinotta, F.A., Ehresmann, B., Wimmer-Schweingruber, R.F., Brinza, D.E., Kang, S., Weigle, G., Böttcher, S., Böhm, E., and 7 co-authors, Measurements of energetic particle radiation in transit to Mars on the Mars Science Laboratory, *Science,* 2013, vol. 340, pp. 1080–1084.
https://doi.org/10.1126/science.1235989